

Supplementary Information

Exploration of CH \cdots π interactions involving the π -system of the pseudohalide coligands in metal complexes of a Schiff-base ligand

Prateeti Chakraborty,^{a,*} Suranjana Purkait,^a Sandip Mondal^a, Antonio Bauzá,^b
Antonio Frontera,^{b,*} Chiara Massera,^c and Debasis Das^{a,*}

^a*Department of Chemistry, University of Calcutta, 92 A. P. C. Road, Kolkata-700 009, India, E-mail: dasdebasis2001@yahoo.com*

^b*Departament de Química, Universitat de les Illes Balears, Crta. De Valldemossa km 7.5, 07122 Palma (Balears), Spain, E-mail: toni.frontera@uib.es*

^c*Dipartimento di Chimica, University of Parma, Parco Area delle Scienze 17/A, 43124 Parma, Italy*

1. FT-IR spectra:

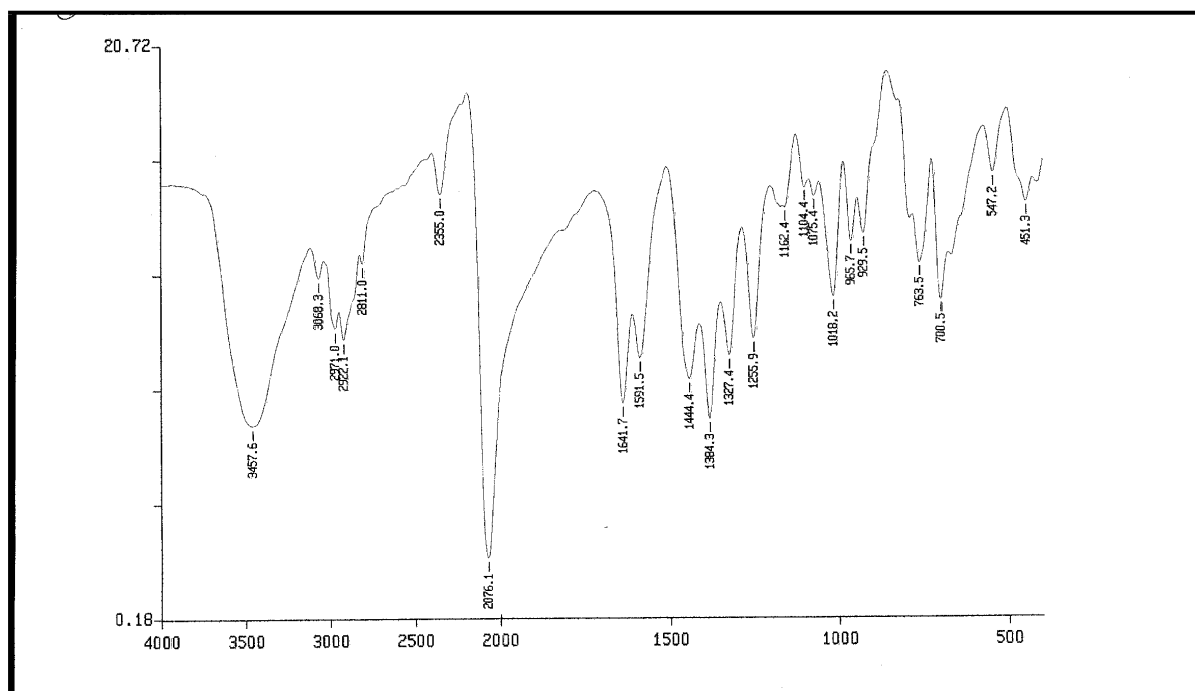


Fig. S1 FT-IR spectrum of complex 1.

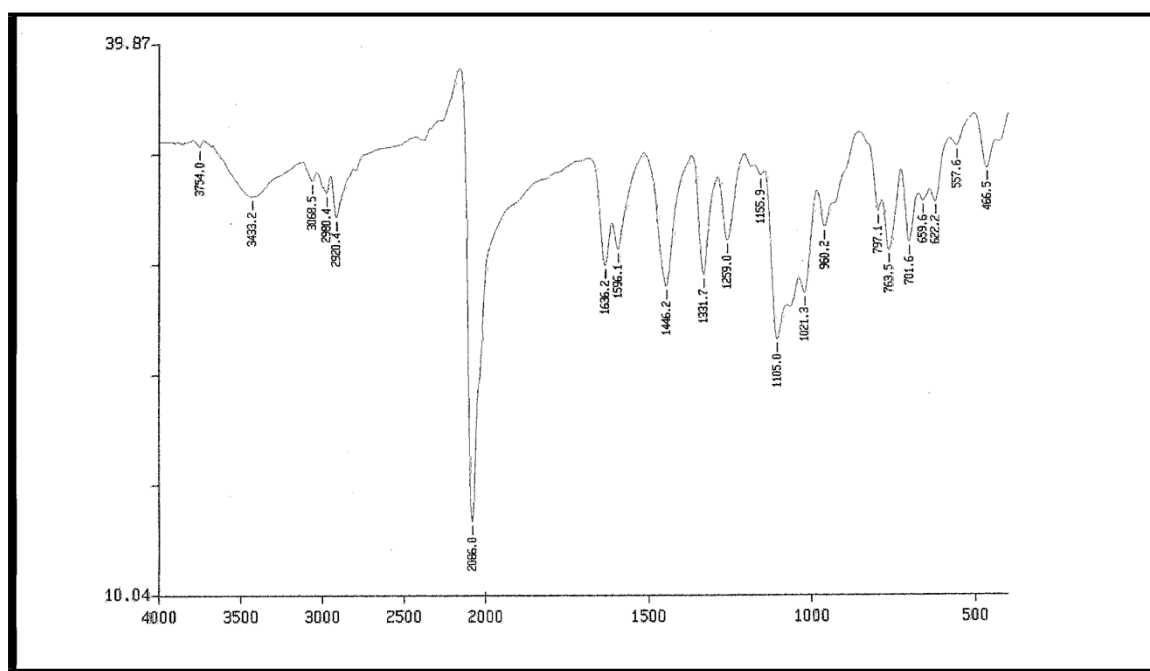


Fig. S2 FT-IR spectrum of complex 2.

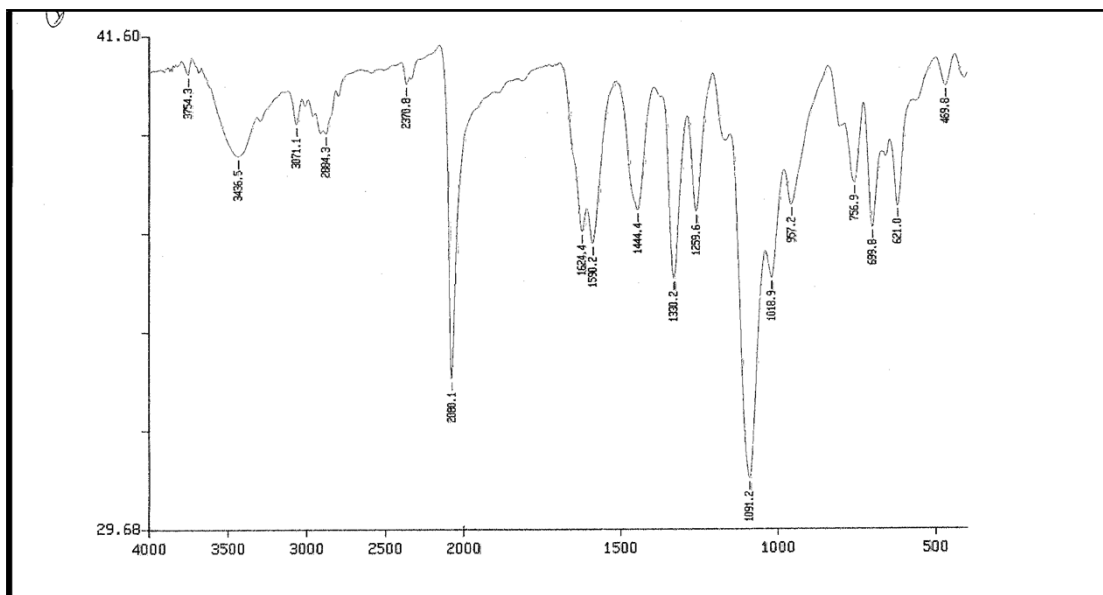


Fig. S3 FT-IR spectrum of complex **3**.

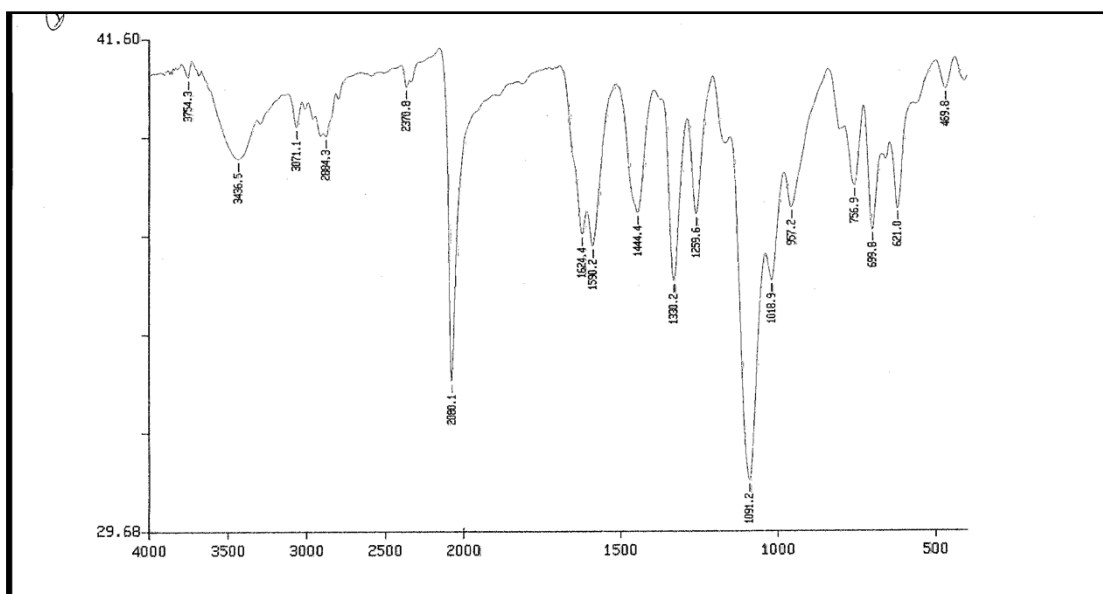


Fig. S4 FT-IR spectrum of complex **4**.

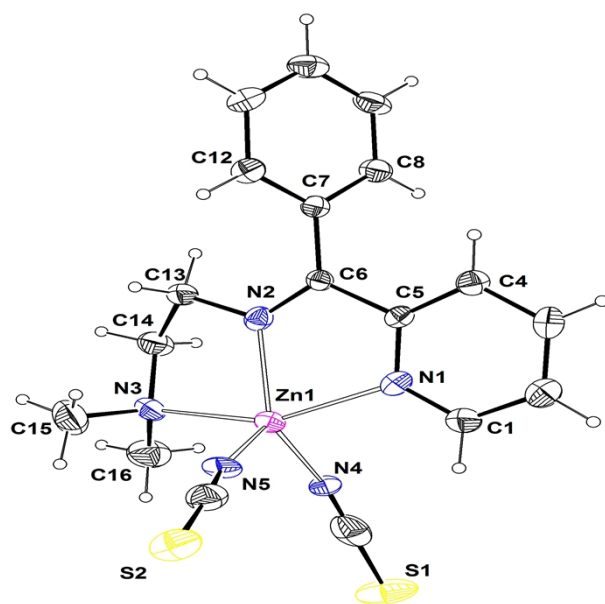


Fig. S5 Ortep view (20% ellipsoid probability) of **1** with partial atom labeling scheme.

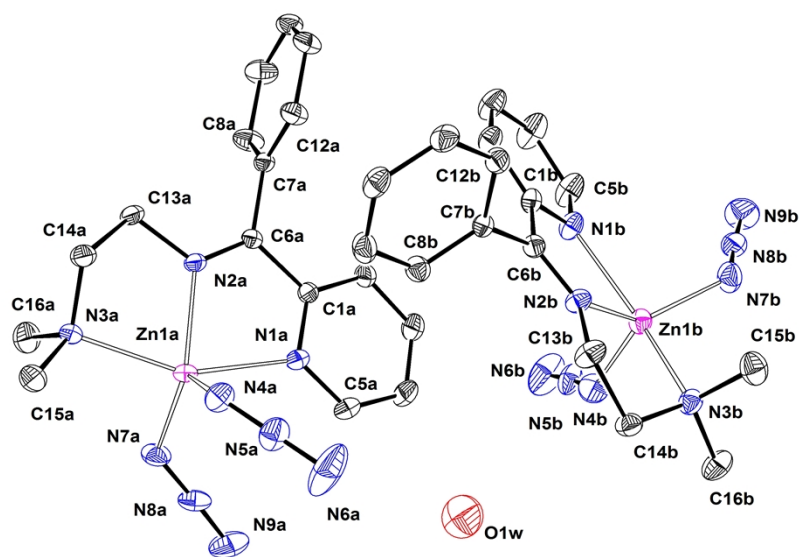


Fig. S6 Ortep view (20% ellipsoid probability) of **2** with partial atom labeling scheme.

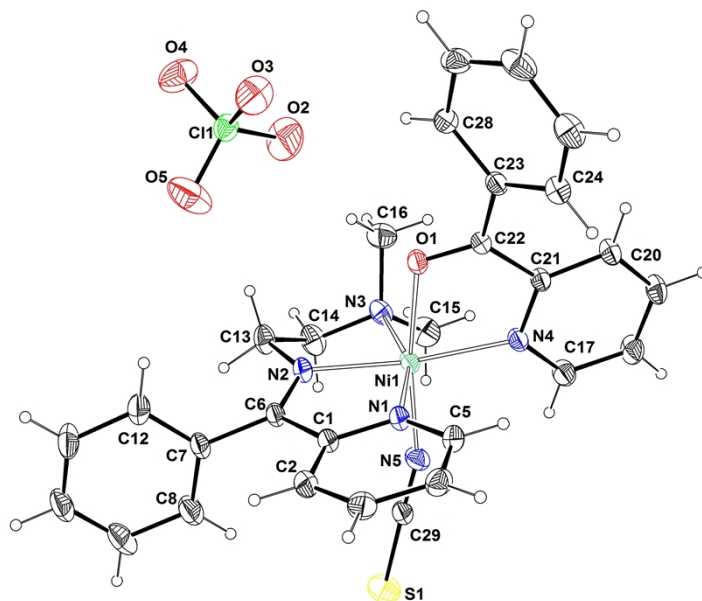


Fig. S7 Ortep view (20% ellipsoid probability) of **4** with partial atom labeling scheme.

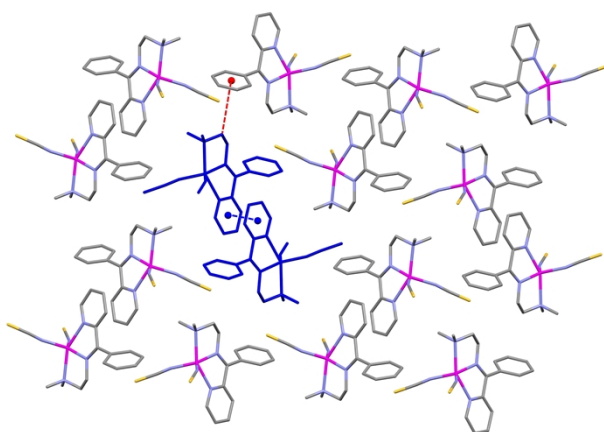


Fig. S8. View along the *a* axis of the relevant supramolecular interactions in the crystal packing of **1**. Two of the dimers formed through $\pi \cdots \pi$ stacking are highlighted in blue. Centroids and interactions are represented as blue and red spheres and dotted lines, respectively. Hydrogen atoms have been omitted for clarity.

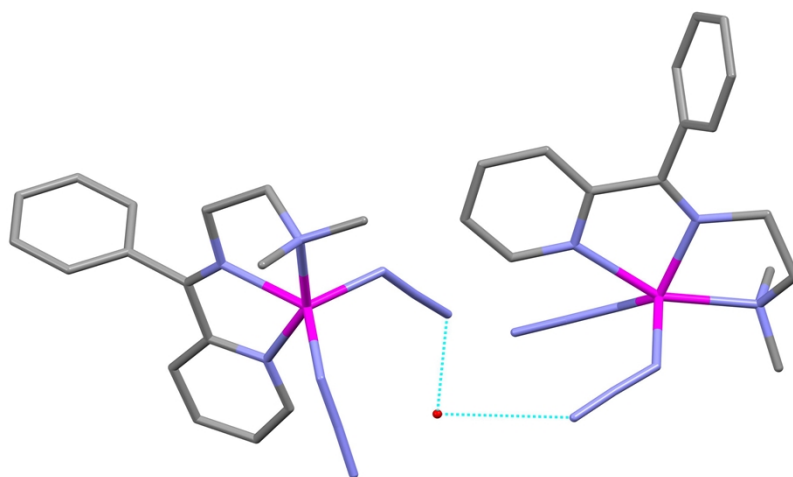


Fig. S9. The two independent complexes in **2**, forming hydrogen bonds (light blue dotted lines) with the lattice water molecule through the terminal azido nitrogen atoms.

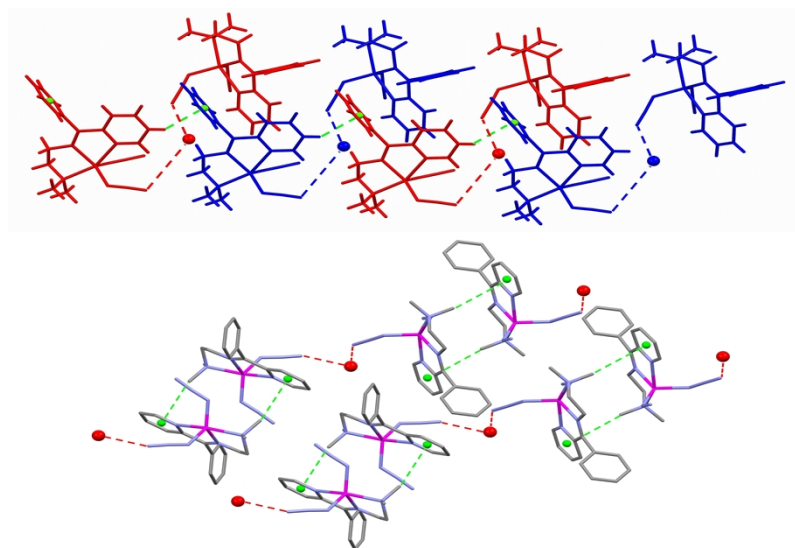


Fig. S10. View of the relevant supramolecular interactions in the crystal packing of **2**. Top: the H-bonded complexes A and B, and the bridging water molecules are highlighted alternatively in blue and red. Hydrogen bonds and C-H \cdots π interactions are represented as dotted lines; centroids are green spheres. Bottom: A \cdots A and B \cdots B dimers.

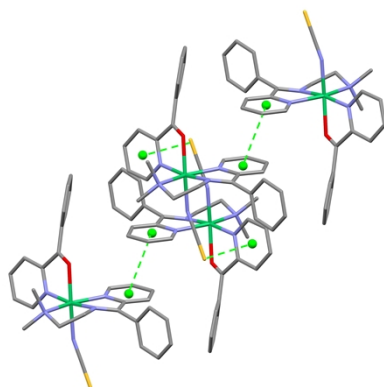


Fig. S11. View of the crystal packing in **4**. $\pi \cdots \pi$ and $S \cdots \pi$ interactions are represented as green dotted lines. Centroids are green spheres. Hydrogen atoms have been omitted for clarity.

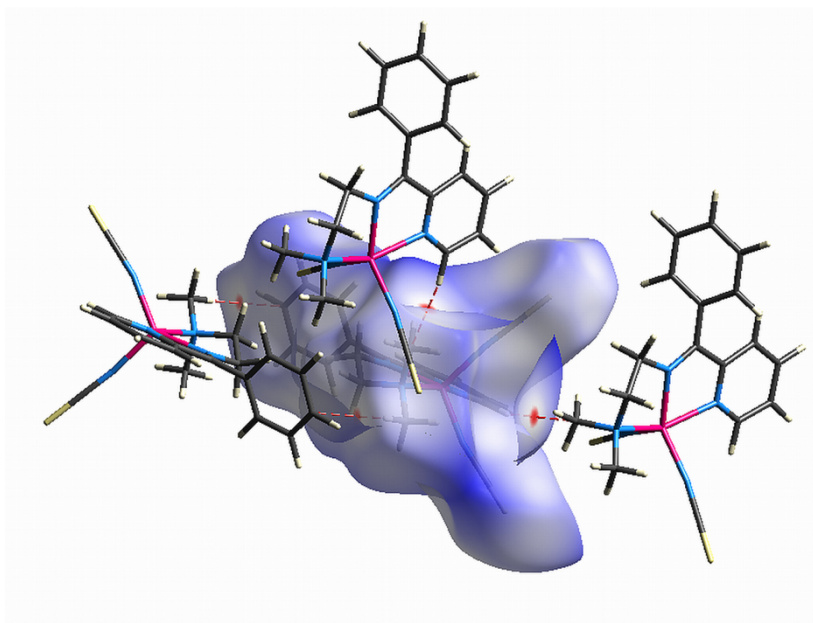


Fig. S12 Hirshfeld surface of **1** mapped with d_{norm} . The $C \cdots H$ interactions are highlighted as red dotted lines.

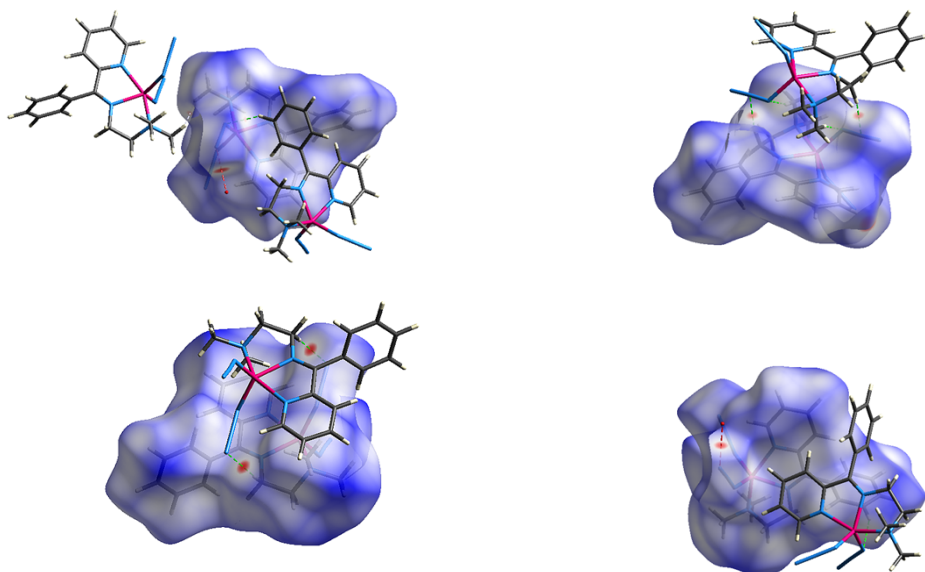


Fig. S13 Hirshfeld surfaces of the two independent complexes of **2** mapped with d_{norm} . Top: Two different orientations of complex A; bottom, two different orientations of complex B. $\text{N}\cdots\text{O}$, $\text{N}\cdots\text{H}$, $\text{H}\cdots\text{H}$ interactions are represented as red, green and grey dotted lines, respectively.

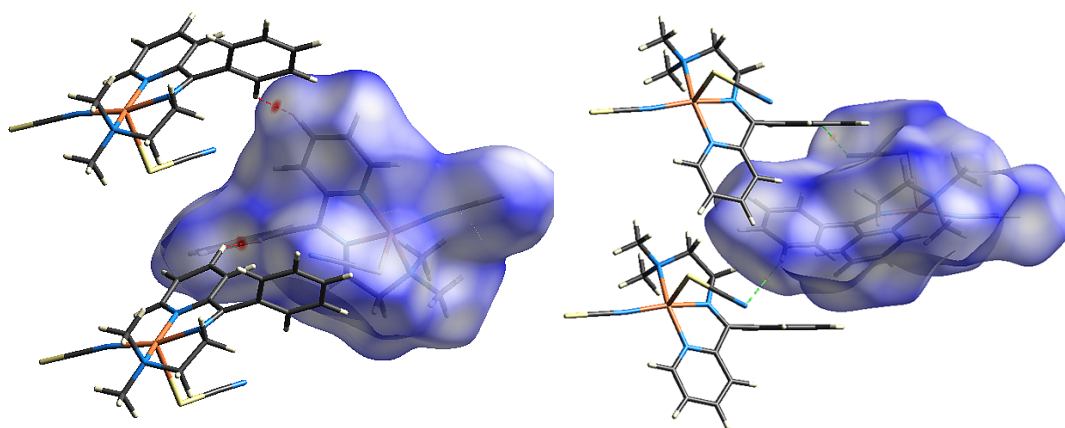


Fig. S14 Hirshfeld surfaces of **3** mapped with d_{norm} . Two different orientations are shown. The $\text{H}\cdots\text{H}$ and $\text{N}\cdots\text{H}$ interactions are highlighted as red and green dotted lines, respectively.

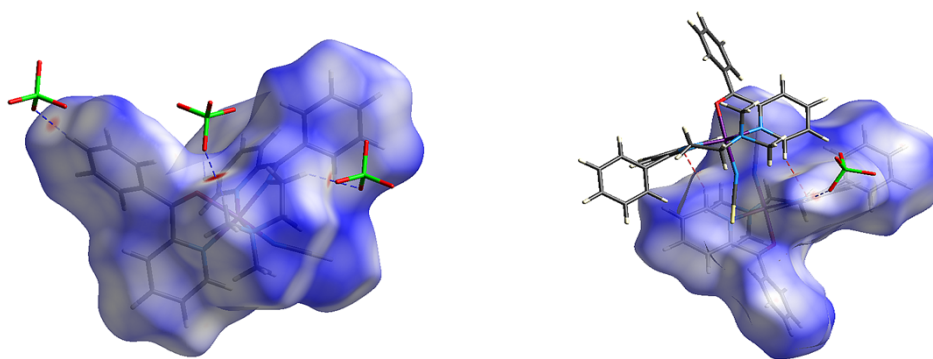


Fig. S15 Hirshfeld surfaces of **4** mapped with d_{norm} . Two different orientations are shown. O \cdots H and C \cdots H interactions are represented as blue and red dotted lines, respectively.

Additional theoretical study for compounds **1** and **2**:

The interaction energies of the additional theoretical models are shown in Fig. S13. In particular, we have computed the interaction energies in hypothetical dimers where the pseudohalide ligands have been replaced by hydride ligands to know the contribution of this peculiar CH \cdots π interaction (where the π -system is provided by the pseudohalide). For compound **1**, this interaction energy (denoted as $\Delta E_1'$) is -3.2 kcal/mol and the difference with ΔE_1 ($\Delta E_1 - \Delta E_1' = -18.1$ kcal/mol) gives the contribution of both CH \cdots π interactions, which is large compared to the π - π interaction. For compound **2** the interaction energy of the dimer where the pseudohalide has been replaced by a hydride is $\Delta E_2' = -14.8$ kcal/mol, therefore each CH \cdots π interaction is $(\Delta E_2 - \Delta E_2')/2 = -6.1$ kcal/mol that is similar in energy to each individual CH $_3\cdots\pi$ interaction ($\Delta E_2'/2 = -7.4$ kcal/mol). These interaction energies are larger than previously reported for conventional C-H/ π interactions that is likely due to the enhanced acidity of the interacting hydrogen atoms due to the coordination to the Zn(II). We have also computed theoretical models of **1** and **2** where the Zn(II) and the pseudohalide counterions have been removed in order to know the influence of the metal center on the π - π stacking and CH $_3\cdots\pi$ interactions. The interaction energies are $\Delta E_1'' = -5.6$ kcal/mol and $\Delta E_2'' = -6.7$ kcal/mol for **1** and **2**, respectively (see Figure 12). Therefore the influence of the metal coordination upon the π - π stacking interaction is small and unfavorable and, conversely its influence in the CH $_3\cdots\pi$ interaction is large and favorable, in agreement with the aforementioned

explanation regarding acidity increase of the hydrogen atoms of the $\text{NR}(\text{CH}_3)_3$ moiety upon coordination.

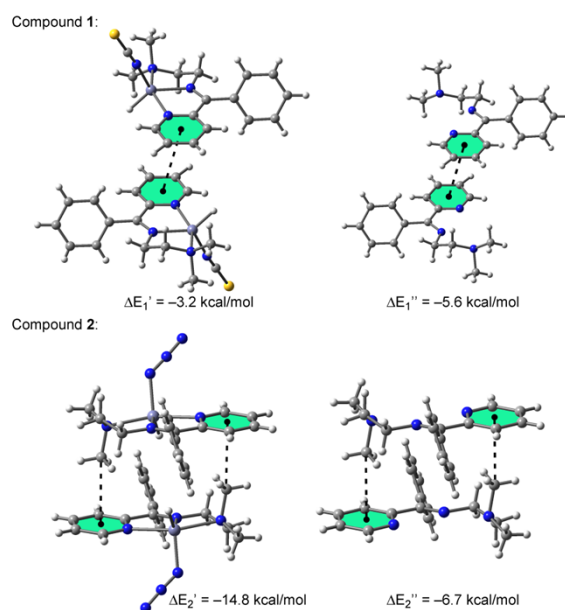


Figure S16. Theoretical models of compounds **1** and **2** and their interaction energies.

In order to further analyze this unconventional $\text{C-H}\cdots\pi$ interaction where the π -system belongs to a pseudohalide anion (Ps^-) coordinated to Zn we have computed the Molecular Electrostatic Potential surface of several $\text{Zn}(\text{Ps})_2$ complexes ($\text{Ps} = \text{N}_3$, NCO , NCS and NCSe) in order to examine the energetic and geometric features of this interaction from an electrostatic point of view. The maps are represented in Figure S14 and interesting issues arise from the inspection of the results. First the electrostatic potential at the central atom of the pseudohalide is positive for N_3 and NCO , and negative for NCS and NCSe , and the contrary is found for the nitrogen atom coordinated to Zn. Second, in N_3 and NCO complexes the global minimum is not found in the region of π -system of the ligand, instead it is located in the prolongation of the $\text{N}\equiv\text{N}$ and $\text{C}=\text{O}$ bonds, for azide and isocyanate respectively, with very similar electrostatic potential energy values. In contrast the global minimum is found in the π -system in thioisocyanate and selenoisocyanato complexes, located in a negative potential belt around the chalcogen atom. In these ligands a σ -hole is found on the outermost portion of the chalcogen surface, centered on the NCCCh axis ($\text{Ch} = \text{chalcogen}$). X-ray structures are in good agreement with the MEP surface results shown in Figure S14 since in compound **2** (azide) the $\text{C-H}\cdots\pi$ interaction involves the

ending nitrogen atom of the ligand and in compound **1** it involves the central C atom that presents a negative value of MEP at the van der Waals surface. Obviously the interaction with the S atom is favored, however the rigidity of the structure and other packing factors influence the final position of the interacting hydrogen atom in **1**.

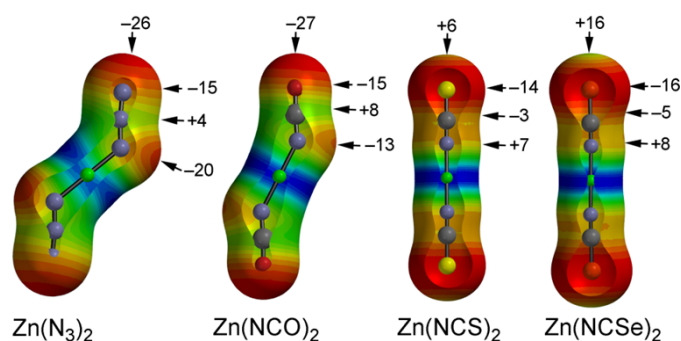


Figure S17. Molecular Electrostatic Potential energy surfaces for several Zn(Ps)₂ compounds. The energies are in kcal/mol.

5. Additional theoretical study for compound **3**:

We have evaluated the energetic difference between the two possible coordination modes of the thiocyanate anion to the Cu atom. The theoretical models used are shown in Fig. S15 (right), where only two ligands have been used to minimize the steric effects that may influence the coordination angle and energy. The most stable geometry is Cu(NCS)₂, where both SCN⁻ ligands are coordinated to Cu through the nitrogen atom in agreement with the CSD analysis that showed a clear preference for this binding mode. The most unfavorable geometry is Cu(SCN)₂ that is 24.9 kcal/mol higher in energy. The mixed Cu(NCS)(SCN) complex is 12.7 kcal/mol higher in energy. The theoretical angles observed in the optimized complexes are also in reasonably agreement with the data retrieved from the CSD (see histogram plots in the main text, Fig 12), which confirm that the Cu–SCN complexes have preference for smaller Cu–S–C angles (~100°) than those in Cu–NCS complexes (~180°). It is important to note that these values are computed free from other influences such as additional interactions (ancillary N/S⋯M or H-bonding interactions) that can be present in the solid state. Therefore there is a significant geometric preference in the coordination angle depending on the binding mode adopted by the SCN ligand.

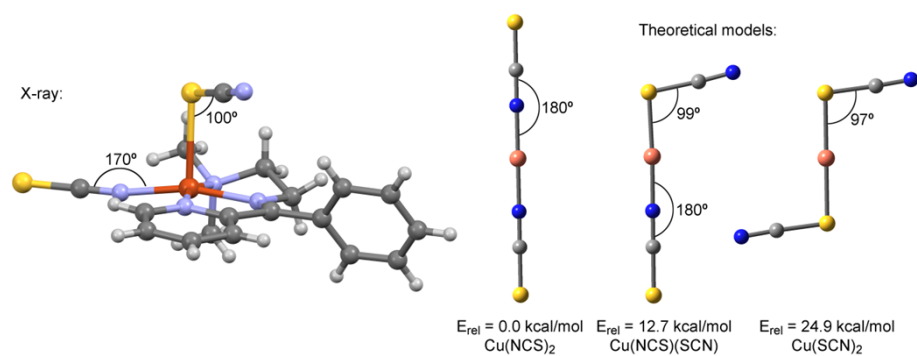


Fig. S18 X-ray structure of compound **3** (left) and the optimized structures of three different isomers of Cu(NCS)₂ (right).

Table S1. Percentage contributions of the different intermolecular contacts to the Hirshfeld surface areas for **1-4**.

	1	2A	2B	3	4
H···H	38,5	35,1	32,9	40,9	44,9
C···H	19,5	16,6	17,3	22,2	22,8
C···C	2	0,6	0,6	1	2,4
N···H	5,3	43,6	41	11,1	1,5
S···H	25,5	-	-	18,7	10
O···H	-	-	4,5	-	16,8
other	9,2	4,7	4,3	6,1	1,6

Table S2. Photophysical parameters of the metal complexes along with the ligand in methanol with excitation at $\lambda = 341$ nm.

	Emission(λ_{\max} in nm)	Quantum Yield
Ligand	457	0.1068
Complex 1	472	0.3529
Complex 2	465	0.3466
Complex 3	464	0.3072
Complex 4	462	0.2168